International Journal of Sciences: Basic and Applied Research (IJSBAR)

ISSN 2307-4531
(Print & Online)

http://gssrr.org/index.php?journal=JournalOfBasicAndApplied

New Cyclotides Isolated from the Roots of *Allexis batangae* (Violaceae)

Ernestine Nkwengoua Tchouboun Zondegoumba[a*], Olivier Ndogo Eteme[b], Celine Nguefeu Nkenfou[c], David Setchaba Kanye[d], Barthélémy Nyasse[e]

[a,b,e]*Department of Organic Chemistry, Faculty of Science, University of Yaounde I, Cameroon*

[c]*Higher Training Teaching School of Yaounde, Molecular Biology Center of Yaounde, Cameroon*

[c]*Chantal Biya International Reference Centre*

[d]*Rhodes University, South-Africa*

[a]*Email: ernestine.nkweng@gmail.com; enkweng@uy1.uninet.cm,* [b]*Email: leptit.neo@gmail.com,*
[c]*Email: kenfou@yahoo.com,* [d]*Email: s.kyanye@ru.ac.sa,* [e]*Email: nyasse2015@gmail.com*

Abstract

Cyclotides are a very abundant class of plant peptides that display significant sequence variability around a conserved cystine-knot motif and a head-to-tail cyclized backbone conferring them with remarkable stability. Their intrinsic bioactivities combined with tools of peptide engineering make cyclotides an interesting template for the design of novel agrochemicals and pharmaceuticals. In this work, we extend the knowledge about their sequence diversity by analyzing the cyclotide content of a Violaceae specie native to Cameroon. Using an experimental approach, which was named sequence fragment assembly by MALDI-TOF/MS, it was possible to characterize 4 cyclotides from the roots of *Allexis batangae*. Amino acid sequencing of various enzymatic digests of cyclotides allowed the accurate assembly and alignment of smaller fragments to elucidate their primary structure.

Keywords: Cyclotides; NMR, Violaceae; *Allexis batangae; Alba1; Alba2; Alba3;*L C-MS; RP-HPLC and MALDI-TOF/MS; Sequence.

---

* Corresponding author.

1. Introduction

Cyclotides are plant-derived, disulphide-rich, mini-circular proteins with a cyclic cystine (CCK) node formed from six cysteine residues on the head-to-tail cyclic skeleton [1]. Typically, cyclotides range in size from 28 to 37 amino acids. They are generally found in plant from Violaceae, Rubiaceae, Fabiaceae, Cucurbitaceae, Fabiaceae [2]. The sequences of some of these cyclotides are presented in table 1. The typical three-dimensional structure with the CCK motif is illustrated with the K1 cyclate prototype B1 [3, 4a, b] Cyclotides are grouped into Möbius or bracelets according to their topology [1]. Möbius cyclotides are identified by the presence of a Cis-Pro residue conserved in loop 5, while those lacking the Cis-Pro bond are called bracelet cyclotides. The presence of a Cis-Pro residue induces a 180 ° twist architecture, a topological entity known as the Möbius band in members of the Möbius subfamily. In addition to this conceptual topological difference, the two sub-families can also be distinguished by their variation in size and loop sequence. With the exception of loop 4, the remaining five loops of members of the Möbius subfamily have at least one conserved residue; in fact, about 60% of the residues are highly conserved [4a]. In contrast, members of the bracelet subfamily have a Glu residue in loop 1 and a Pro terminal in loop 2 that are highly conserved [4b]. According to studies made by R. Hellinger and his colleagues 2015, the overall number of unique cyclotides to be discovered in plants has been estimated to exceed 100,000 [5]. *Allexis batangae*, a plant belonging to the Violaceae family is commonly found in Cameroon [6]. Violaceae plants; a main sources of cyclotides have been constantly used in Cameroonian traditional folk to treat many diseases caused by pathogenic agents. Studies done by R Burman and his colleagues in 2015 estimate 5000-25000, the number of different cyclotides in the Violaceae family [7]. In our knowledge, no research work has been published on cyclotide from Violaceae family. Herein, we report the isolation and structural elucidation of four cyclotides from the roots of *Allexis batangae*.

2. Material and methods

2.1. Harvest

Allexis batangae was harvested on 7 June 2014 in Bidou II, 20 km from the city of Kribi (South Cameroon) under the supervision of a Botanist (Mr. NANA). The identification was carried out at the National Herbarium of Cameroon in comparison with the specimen number 31839 / HNC.

2.2. Extraction Methods

Dry/fresh plant material was ground to powder using a mortar and pestle by adding liquid N2 and extracted with dichloromethane (DCM) / methanol (1:1(v/v)) overnight at room temperature. Debris from the extraction was removed by filtering through cotton wool/filter paper and transferred into a separating funnel. Appropriate amount of Milli-Q water was added until a clear separation was obtained between DCM and aqueous methanol layers. The top aqueous methanol layer was collected and the methanol was removed on a rotary evaporator followed by lyophilisation. All the lyophilised extracts were stored at -20oC for further analyses.

2.3. Identification and analyses of cyclotides

The identification, isolation, purification and characterization of cyclotides from *Allexis batangae* was carried out using combinations of LC-MS, RP-HPLC and tandem mass spectrometry [7,8] as illustrated in Figure 1 below.

ABREVIATIONS

Table 2

Ala (A):	alanine
Asn (N):	asparagine
Arg (R):	arginine
Asp (D):	aspartic acid
CCK:	cyclic cystine knot
CHCA:	α-cyano-4-hydroxycinnamic acid
cryo-TEM:	Cryogenic transmission electron microscopy
Cys (C):	cysteine
Da:	Dalton
DTT:	dithiothréitol
DMC:	dichloromethane
ESI-MS:	electrospray ionization-Mass spectrometry
Glu (E)–C:	glutamic acid-cysteine
Gln (Q):	glutamine
Gly (G):	glycine
His (H):	histidine
Ile (I):	isoleucine
KB1:	Kalaba B
K.d:	dissociation constant
KV:	kilo volt
LC/MS:	liquid chromatography/ mass spectrometry
Leu (L) :	leucine
LUVs:	large unilamellar visicles
Lys (K) :	Lysine
MALDI-TOF-MS:	matrix-assisted laser desorption ionization time-of-flight mass spectrometry
Met (M):	methionine
NMR:	nuclear magnetic resonance
NOESY :	Nuclear overhauser spectroscopy
Phe (F):	phenylalanine
P.L:	peptide-to-liquid molar ratios
Pro (P):	Proline
POPA:	1-palmitoyl-2-oleoyl phosphatic acid
POPC:	1-palmitoyl-2-oleoyl-*sn*glycero-3-phosphocholine
POPE:	1-palmitoyl2-oleoyl-*sn*-glycero-3-phosphoethanolimine
RP-HPLC	Revere Phase high performance liquid chromatography
POPG:	1-palmitoyl-2-oleoyl phosphatidyl glycerol
Ser (S):	Serine
SPR :	Surface plasmon resonance
TCEP:	tris (2-carboxyethyl) phosphine Chlorhydrate
TOCSY:	total correlation spectroscopy
Trp (W):	Tryptophan
Tyr (Y):	Tyrosine
RP-HPLC:	RP-high performance Liquid chromatography
SUVs:	small unilamellar visicles
Val (V):	valine

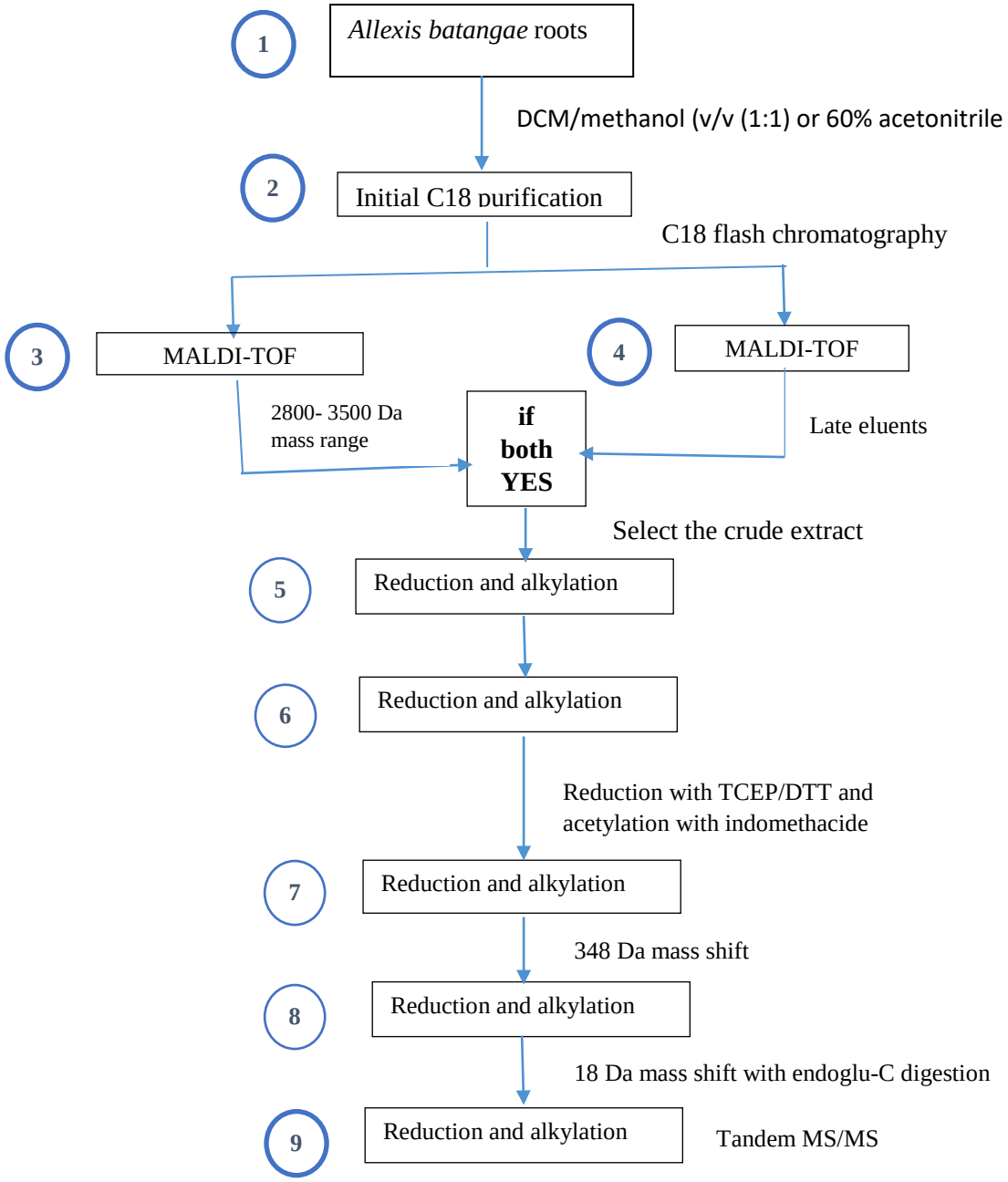

Figure 1: Schematic diagram illustrating the screening of the roots of *Allexis batangae* plant for the presence of cyclotides.

2.4. LC-MS analysis of cyclotides

The dry extracts were resuspended in 10% acetonitrile consisting 1% (v/v) trifluoroacetic acid and separated on a Phenomenex C18 RP-HPLC column (150 X 2.00 mm, 3 microns, 300 Å) with a linear 1% min^{-1} acetonitrile gradient (0 to 80 % solvent B which consists of 90% acetonitrile and 0.5% formic acid) at a flow rate of 0.3 mL min^{-1} on Schrimadzu LC-MS 2020.The eluents were monitored on a dual wavelength UV detector set to 214 and 280 nm. The mass spectra of all LC samples were obtained in positive ion mode with a mass range of *m/z* 400 – 2000 Da.

2.5. MALDI-TOF analysis

The molecular weights of all cyclotides characterized in this work were determined by matrix assisted laser desorption/ionization time-of-flight mass spectrometry (MALDI-TOF-MS) on a 4700 Proteomics Analyzer (Applied Biosystems). The peptide samples were reconstituted in 50% acetonitrile and diluted at 1:1 ratio with CHCA (α-cyano-4-hydroxycinnamic acid) matrix prepared at 5-6 mg/mL in 50% (v/v) acetonitrile and 2% (v/v) formic acid. One – two µL of peptide matrix mixture was spotted onto a stainless steel MALDI plate and dried in presence of liquid N2 or room temperature. The MALDI spectra of samples were acquired with the following conditions and spectra were analyzed on Dataone explorer 4.1 software.

Operating mode: Reflector positive mode

Source voltage: 20kV

Mass range: 1000 – 4000 Da

Focus mass: 3000 Da

Laser shots: 1000 - 2000

Laser intensity: 2500 – 3500

2.6. Purification of cyclotides

Dried solvent extracts were suspended in approximately 20% (v/v) acetonitrile containing 2% (v/v) formic acid and separated on a Phenomenex C18 RP-HPLC column (250 X 21.00 mm, 10 microns, 300 Å) with a flow rate of 8 mL min^{-1} at linear 1% min^{-1} acetonitrile gradient. Eluents were collected into individual test tubes of 10 mL capacity at 1-minute interval between 20 min and 83 min. All the fractions were analyzed for cyclotide like masses on Applied Biosystems 4700. The fractions containing cyclotide like masses were pooled together and lyophilized. The lyophilised peptide samples were suspended in 20% (v/v) acetonitrile containing 2% (v/v) formic acid and separated on a Phenomenex C18 RP-HPLC column (250 X 10 mm, 5 microns, 300 Å) with a flow rate of 3 mL min^{-1}. The pure peptides were collected manually based on UV absorbance at 214 nm and 280 nm. Purity of collected samples was analyzed on MALDI-TOF-MS. (v/v) formic acid and separated on a Phenomenex C18 RP-HPLC column (250 X 21.00 mm, 10 microns, 300 Å) with a flow rate of 8 mL min^{-1} at linear 1% min^{-1} acetonitrile gradient. Eluents were collected into individual test tubes of 10 mL capacity at 1-minute interval between 20 min and 83 min. All the fractions were analyzed for cyclotide like masses on Applied Biosystems 4700 as described above. The factions containing cyclotide like masses were pooled together and lyophilized. The lyophilized peptide samples were suspended in 20% (v/v) acetonitrile containing 2% (v/v) formic acid and separated on a Phenomenex C18 RP-HPLC column (250 X 10 mm, 5 microns, 300 Å) with a flow rate of 3 mL min^{-1}. The pure peptides were collected manually based on UV absorbance at 214 nm and 280 nm. Purity of collected samples was analyzed on MALDI-TOF-MS. The pure cyclotides were freeze-dried and stored at -20^{0}C for further studies including *de novo* characterization, biological activities and mode of

action studies.

2.7. Reduction, alkylation and enzymatic digestion

Approximately 50 µM of lyophilized pure dry peptide was reconstituted with 40 µL of 100 mM Na_2HCO_3 and mixed on vortex. The CCK motif of native cyclotides was unknotted by addition of 5 µL of 0.1 M DTT prepared in deionized water and incubated at 37^{o}C for one hour. The free thiol groups were capped with carboxymethyl amine by addition 5 µL of 0.1 M iodoacetamide prepared in DIO and incubated at room temperature. Desalting of reduced and alkylated cyclotides was carried out using C18 Ziptips (Millipore). The modifications in reduced and alkylated cyclotides were analyzed on MALDI-TOF-MS

*2.8. De novo sequencing of cyclotide***s**

The reduced and alkylated cyclotides were digested using individual proteolytic enzymes including endoGlu-C, trypsin and chymotrypsin or combinations of these enzymes. Each individual digest was performed by addition of 1 µL of 500 ng of enzyme to 10 µL of aliquot of reduced and alkylated cyclotide followed by incubation at 37^{0}C for 3-4 hrs. The digested peptide samples were desalted using Ziptips (Millipore) followed by analysis on MALDI-TOFMS.

The reduced and alkylated samples were subjected to MS/MS analysis using a Qstar Pulsar mass spectrometer (Applied Biosystems). Approximately, 5-7 µL of desalted peptide reconstituted in 80% acetonitrile 2% formic acid loaded into Proxeon nanospray tips and TOF-MS and MS/MS spectra were acquired applying the following conditions.

Capillary voltage: 800 – 1000 Volts

Collision energy: 10 – 50 Volts

TOF MS spectra (m/z): 500 – 2000 Da

TOF MS/MS spectra (m/z): 100 – 2000 Da

TOF-MS and MS/MS spectra were analyzed on Analyst QS 1.1 Software. The *de novo* sequence was attained based on b-series and y-series ions.

2.9. Quantification of lysines using acetylation

The number of Lys-residues in the normal cyclotides was quantified based on acetylation experiments. Acetylation reagent was freshly prepared with 20 µL acetic anhydride and 60 µL methanol. Approximately 15-20 µg of dry peptide was reconstituted in 20 µL of 50 mM ammonium bicarbonate. Acetylation reagent (50 µL) was added to 20µL of peptide solution and incubated at room temperature for one hour followed by lyophilisation to remove organic content. The samples were desalted using ziptips and the acetylation products were analyzed on MALDI-TOF-MS) on a 4700 Proteomics Analyzer (Applied Biosystems). Acetylation of

peptides results in addition of acetyl group to free Nterminior Lys-residues. Cyclotides feature a head-to-tail cyclic backbone, and hence they lack free N-termini. The results of a mass increment of 42 Da to native cyclotide mass, suggests the presence of one Lys as described below. III-10- Membrane binding affinity of cyclotides

2.10. Membrane binding affinity of cyclotides

In order to evaluate the lipid specificity, pure peptide solutions and various complex lipid mixtures were prepared to mimic the natural composition of biological membranes. The affinity of cyclotides towards biological membranes was evaluated on model membranes composed of synthetic lipids including POPC, POPG, POPA and POPE at different molar ratios. All the lipids were purchased from Avanti Polar Lipids, Inc. POPC was used as a major component of lipid mixtures as it maintains fluid properties at room temperature, which mimics the fluid phase of mammalian cell membranes. Large unilamellar vesicles (LUVs; 100 nm in diameter) were used for fluorescence measurements and cryo-TEM imaging, whereas small unilamellar vesicles (SUVs of 50 nm diameter) were used for SPR studies [9].

In order to evaluate the lipid specificity, pure peptide solutions and various complex lipid mixtures were prepared to mimic the natural composition of biological membranes. The affinity of cyclotides towards biological membranes was evaluated on model membranes composed of synthetic lipids including POPC, POPG, POPA and POPE at different molar ratios. All the lipids were purchased from Avanti Polar Lipids, Inc. POPC was used as a major component of lipid mixtures as it maintains fluid properties at room temperature, which mimics the fluid phase of mammalian cell membranes. Large unilamellar vesicles (LUVs; 100 nm in diameter) were used for fluorescence measurements and cryo-TEM imaging, whereas small unilamellar vesicles (SUVs of 50 nm diameter) were used for SPR studies.

3. Results and discussion

The analyses of the extract from *Allexis batangae* roots led to the isolation of four cyclotides named Alba1, Alba2, Alba3 and Alba4.

3.1. Identification of Alba1

In the present study, the following characteristics were taken into account to confirm that the peptides identified were cyclotides: molecular weight range (2,800 to 3,500 Da), three disulfide bridges formed by six cysteines, back-to-back cyclic dorsal. Figure 2 presents the ESI-MS spectra of Lys-rich Alba1 cyclone (upper panel) showing peaks corresponding to 2+ to 5+ due to increased protonation at additional basic residues with peaks corresponding to dual charge and triple charge ions commonly observed for cyclotides. Figure 2b presents the quantification of Lys by acetylation. MALDI-TOF-MS before acetylation (upper panel) and after its acetylation with acetic anhydride (lower panel) detailing the observed mass displacement.

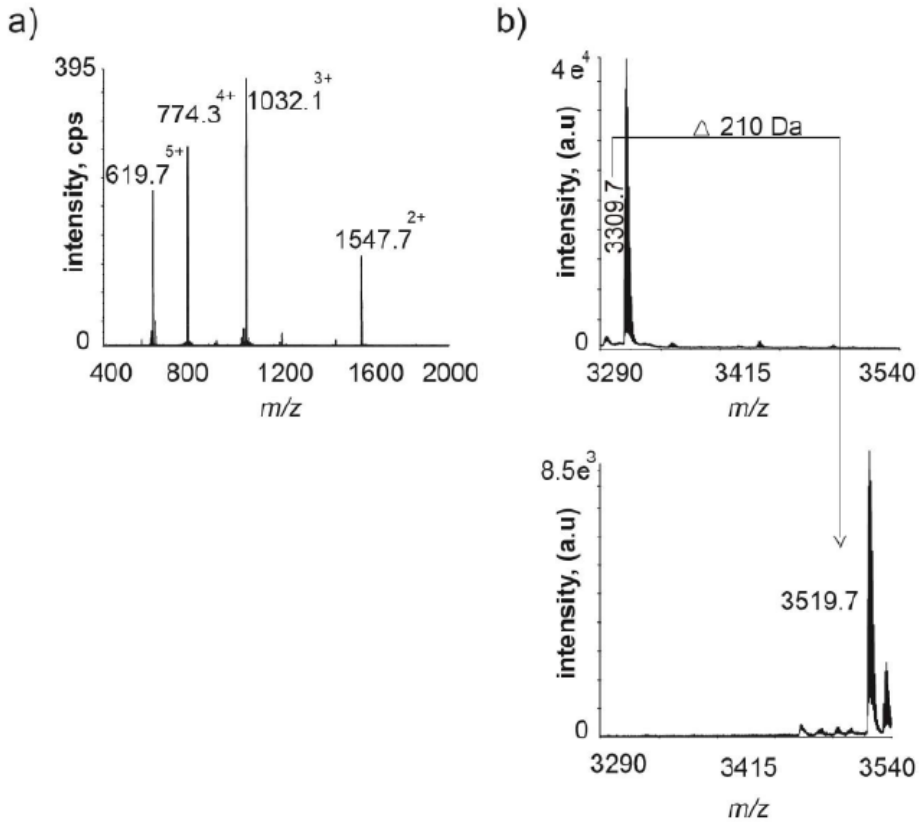

Figure 2: State of charge of Alba1 and quantification of Lys residues. a) ESI-MS spectra of Alba1 (top panel) showing peaks corresponding to 2^+ through to 5^+ as a result of increased protonation at the additional basic residues observed for cyclotides. b) Quantification of Lys through acetylation.

Reduction and alkylation of Alba1 (3092.4 Da) resulted in a mass increase of 348 Da, showing three disulfide bonds. The signal observed at 3459.8 Da after digestion with endoGlu-C indicated an additional 18 Da increment, consistent with cleavage of the peptide backbone and the presence of a single Glu (Figure 3a). The resulting linear peptide was subjected to MS / MS nanospray for de novo sequence determination. MS / MS fragmentation of linearized Alba1 revealed that its sequence was TCFKGKCYTPGCTCSYPLCKKDGKPTCGE (Figure 3b). This sequence contains five Lys residues, which is unusual compared to the positively charged 0-2 residues of conventional cyclotides, but corresponds to the decreased hydrophobicity of the Albal parent (Colgrave and his colleagues 2010). It should be noted that the MS in tandem alone does not distinguish isobaric residues Lys / Gln and Ile / Leu. Thus, enzymatic digestion and side chain modification were used to distinguish these residues and unambiguously characterize the peptide. Tryptic digestion was further carried out on reduced and alkylated cells, producing three main fragments with the sequences CYTPGCTCSYPLCK (1765.9 Da) (Figure 3c), KDGKPTCGETCFK (1526.8 Da) (Figure 3d) and DGKPTCGETCFKGK (1583, 8 Da). By combining these fragments, the complete sequence of Alba1 was obtained, consistent with sequencing of the peptide observed after endoGlu-C digestion and confirming the presence of four of the five Lys residues in the molecule. To assign the isobaric residues (Leu / Ile in loop 5 and

Lys / Gln in loop 6), the ratio of these residues was determined by amino acid analysis (AAA) and AAA showed only one Ile / Leu was a Leu. The precise number of Lys residues was determined by acetylation, which resulted in the modification of the ε-amino ends of the Lys and N termini free side chains. Unlike linear peptides, acetylation leads to the modification of Lys side chains only, resulting in a mass increase of 42 Da per Lys. In addition, amino acid analysis of isolated native peptides revealed amino acid ratios consistent with those obtained with de novo AAA sequencing.

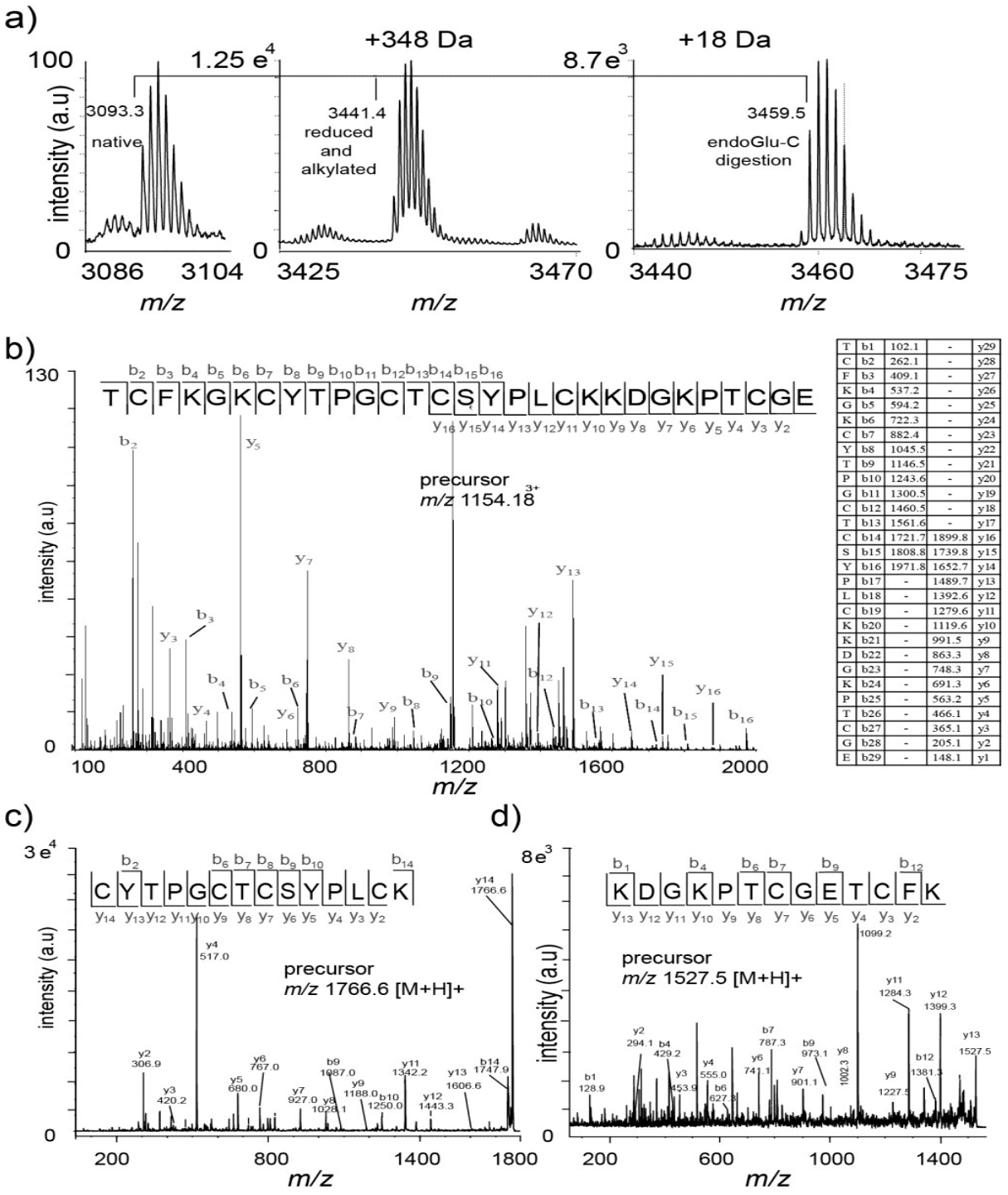

T	b1	102.1	-	y29
C	b2	262.1	-	y28
F	b3	409.1	-	y27
K	b4	537.2	-	y26
G	b5	594.2	-	y25
K	b6	722.3	-	y24
C	b7	882.4	-	y23
Y	b8	1045.5	-	y22
T	b9	1146.5	-	y21
P	b10	1243.6	-	y20
G	b11	1300.5	-	y19
C	b12	1460.5	-	y18
T	b13	1561.6	-	y17
C	b14	1721.7	1899.8	y16
S	b15	1808.8	1739.8	y15
Y	b16	1971.8	1652.7	y14
P	b17	-	1489.7	y13
L	b18	-	1392.6	y12
C	b19	-	1279.6	y11
K	b20	-	1119.6	y10
K	b21	-	991.5	y9
D	b22	-	863.3	y8
G	b23	-	748.3	y7
K	b24	-	691.3	y6
P	b25	-	563.2	y5
T	b26	-	466.1	y4
C	b27	-	365.1	y3
G	b28	-	205.1	y2
E	b29	-	148.1	y1

Figure 3: De novo Sequencing of Alba1

(a)MALDI-MS ofAlba1 from native digestion, reduction and alkylation and endoglu-C (b) ESI-MS / MS digestion of a reduced, alkylated and endoGlu-C digested precursor of alba1 (m / z 1154.183+, 3459.54.2 Da) (c) MALDI-MS / MS precursor ion at m / z 1766.6 and (d) MALDI-MS / MS precursor ion at m / z 1527.5 obtained from a tryptic digestion. The sequence was deduced from the series of ions b and y. The chemical shifts of Alba1 measured with the TOCSY and NOESY NMR spectra are similar to those of the prototypical Möbius kB1 suggesting that they have similar three-dimensional structures.

Series of ions b and y: The chemical shifts of Alba1 measured with the TOCSY and NOESY NMR (Figure 4) spectra are similar to those of the prototypical Möbius kB1 suggesting that they have similar three-dimensional structures.

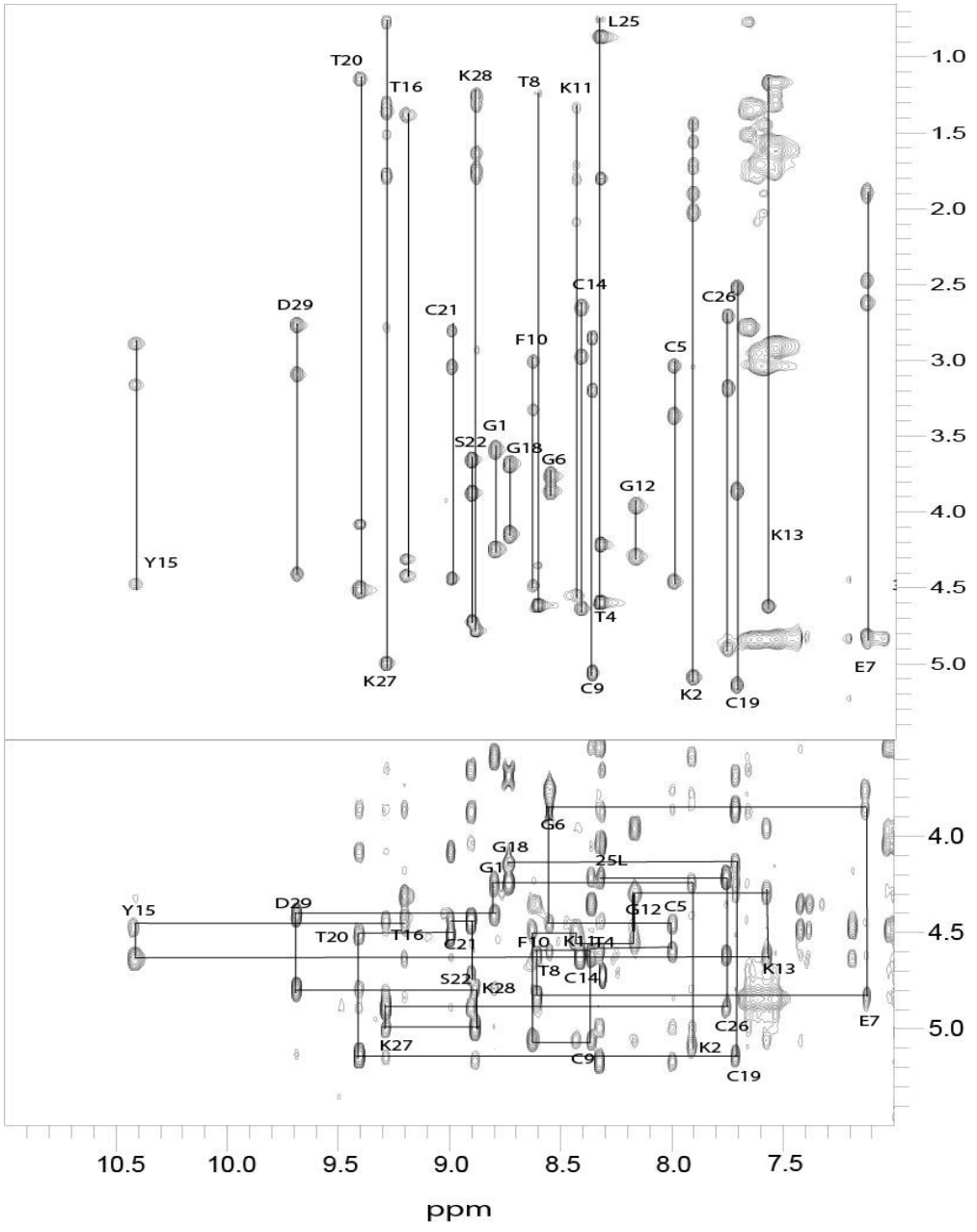

Figure 4: TOCSY and NOESY spectrum of Alba1

Then, ***De novo*** **of Sequence Alba1 is GKPTCGETCFGKKCYTPGCTCSYPLCKKD**

Modeling studies of Lys-rich cyclotides based on chemical shifts indicate that they also exhibit bioactive and hydrophobic spots on their surface, suggesting a similar mode of membrane binding. An earlier binding study using micelles of kB1 and DPC, controlled by NMR spectroscopy, suggested that the hydrophobic patch fits into the hydrophobic core of the membrane and another study suggested that the bioactive patch, particularly Glu 7 conserved, is involved in the targeting of PE lipids (Figure 5).

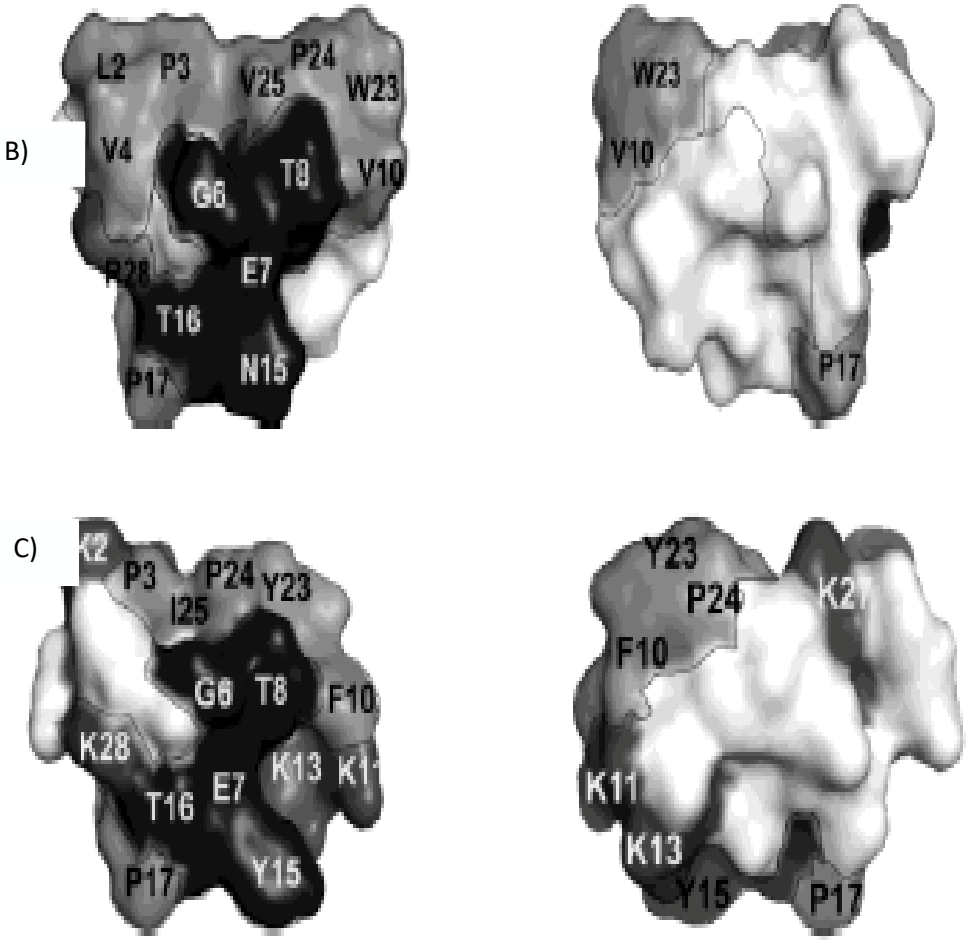

Figure 5: NMR and modeling studies of Lys-rich cyclotides. (A) The overlapping of relative peaks (for all residues except HN-Hα and Hδ2-Hδ3 of Pro) of kB1 with Alba1. (B) Structural models of Alba1 based on kB1 structure

3.2. Identification of Alba2

It exhibits resistance to enzymatic cleavage by trypsin, which is consistent with the presence of a cyclic cystine node pattern characteristic of all cyclotides. After reduction and alkylation, each reduced and 5-aminoethylated cysteine contributes to an increase in molecular weight of 44 Da. A strategy that includes both enzymatic digestion and MS-MS fragmentation was used to complete the sequence analysis of Alba2 as detailed in figure 6 below.

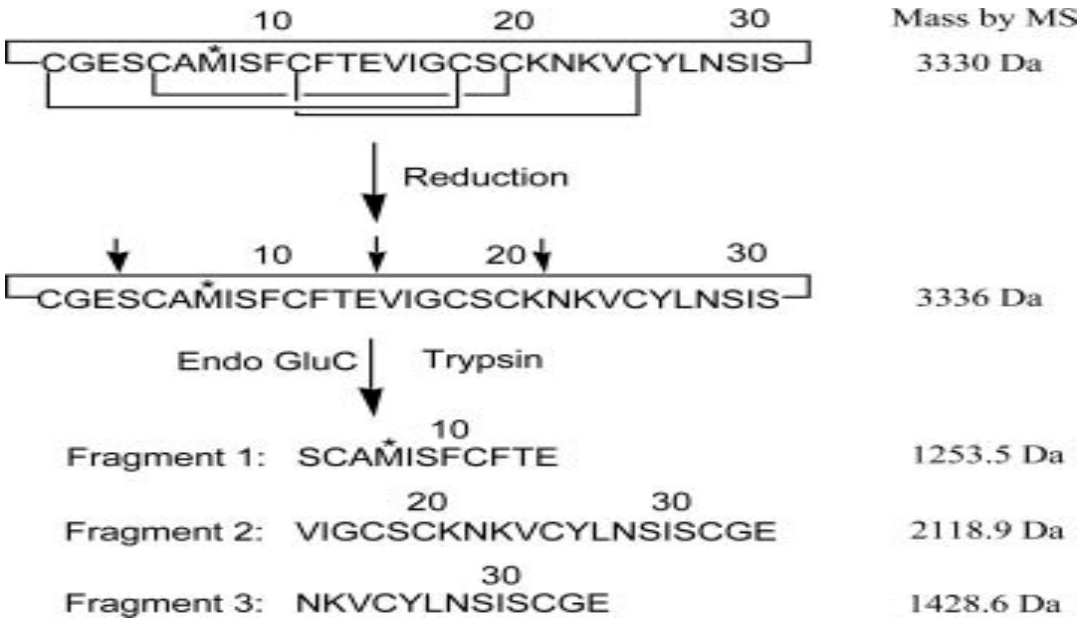

Figure 6: Sequence analysis of Alba2

The native cyclotide was reduced by TCEP and subjected to enzymatic digestion directly, without alkylation of the cysteines. The reduction of the peptide was confirmed by the observation of m / z peaks 1112^{3+} and 834^{4+}, which corresponds to a molecular mass of 3336 Da following the addition of six protons to the native peptide. Digestion of the reduced peptide with endo-GluC resulted in two major peaks at m / z 627.7^{2+} and 707.3^{3+} corresponding to two mass fragments of 1253.5 and 2118.9 and involving the presence of two residues of glutamic acid. Several other relatively low intensity peaks have also been produced after digestion with trypsin or a combination of trypsin and endo-GluC. The MS-MS fragmentation study of the first fragment at m / z 627.7^{2+} resulted in the completion of its amino acid sequence as shown in Figure 7 suggesting that it consists of 11 amino acid residues of the SCAF * ISFCFTE sequence.

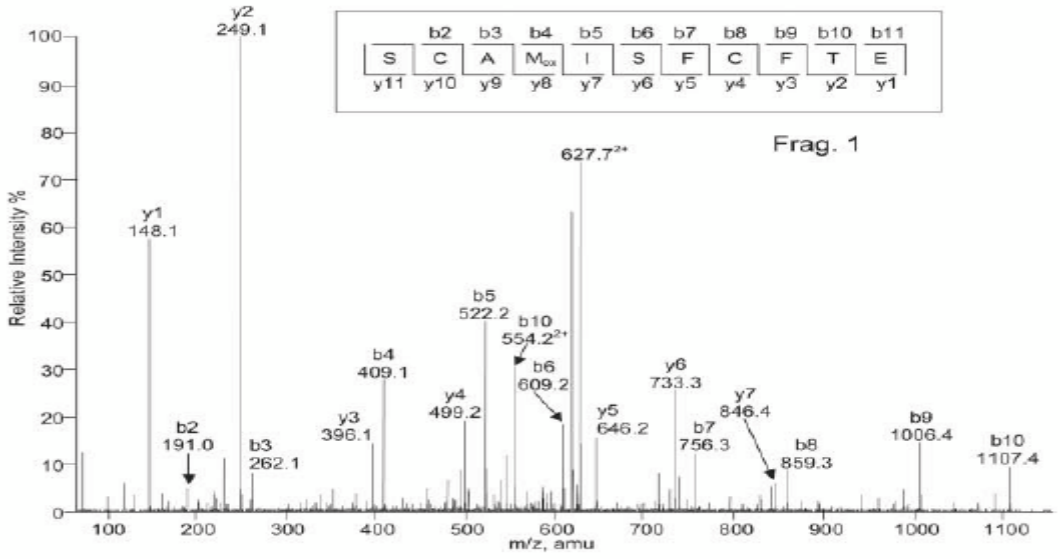

Figure7: MS / MS spectrum of the first fragmentation of Alba2

The b2 ion of the m / z 191 fragment is SC, determined by comparison with known cyclotides. The second m / z 707.33+ fragment was difficult to analyze by MS-MS fragmentation because of its length. However, two partial sequences of both N-terminal (VIGCSCKNKV) and C-terminal (LNSISCGE) ends were observed, as shown in Figure 8 below.

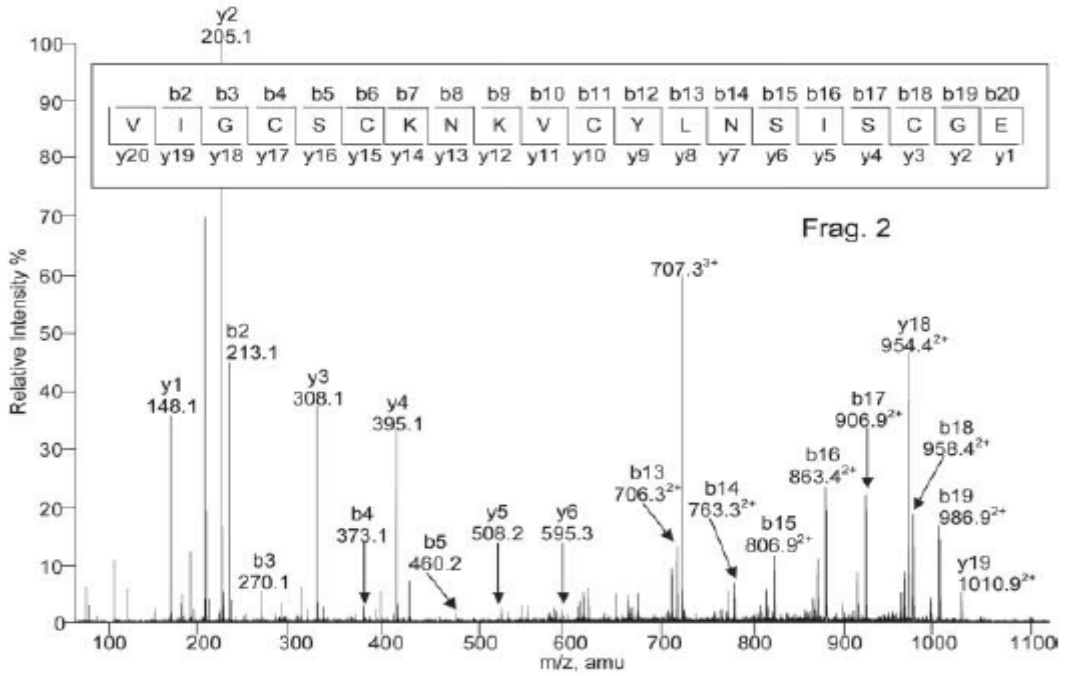

Figure 8: MS / MS spectrum of second fragmentation of Alba2

The third fragment resulting from enzymatic digestion with trypsin and endo-GluC at m / z 715.3^{2+} was subject to MS-MS fragmentation see figure 8 and the sequence NKVCYLNSISCGE was deduced which possessed the information on the N-terminal. The combination of the two sub-fragments led to the sequence VIGCSCKNKVCYLNSISCGE (m/z 707.3^{3+}). See Figure 9 bellow.

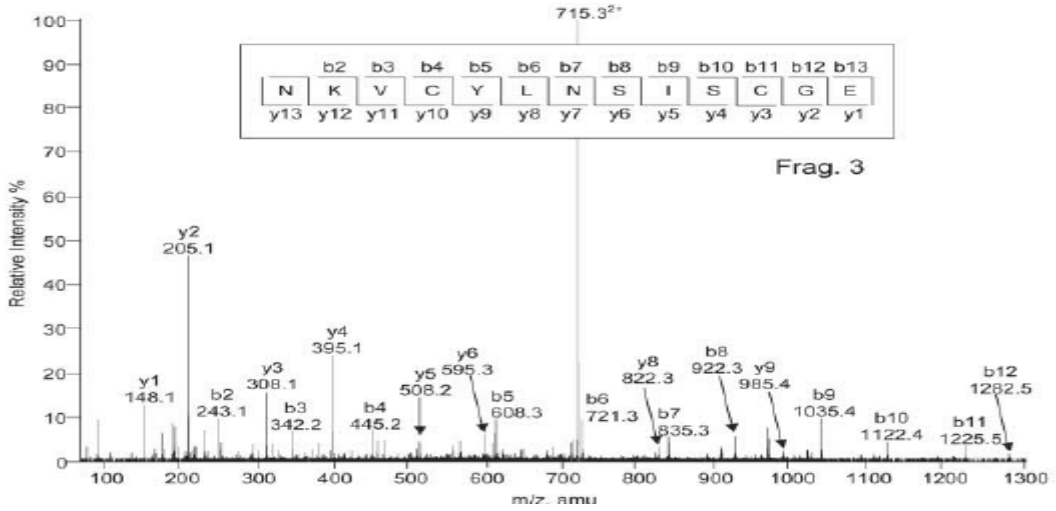

Figure 9: MS / MS spectrum of the third fragmentation of Alba2

The mass difference between b4 and b3 ions of fragment 1 is 147 Da, which suggests that the amino acid residue is Phe. However, according to the two-dimensional spectrum analysis TOCSY and NOESY (Figure 10 and Figure 11), the spin system of this residue shows the presence of two beta and gamma protons, none of which have any correlation with aromatic protons.

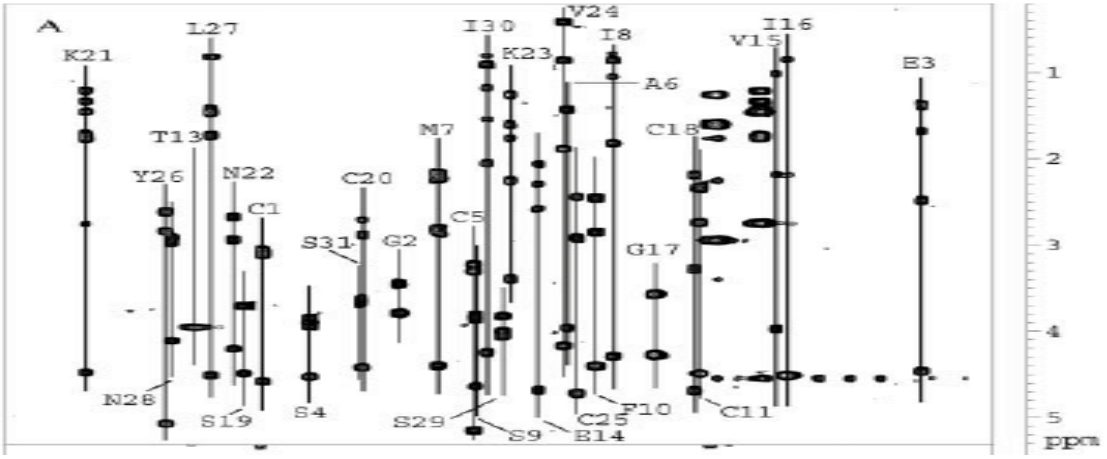

Figure 10: TOCSY spectrum of Alba2

This conclusion is fully consistent with the results of amino acid analysis and "sequential run" in NOESY spectra. As shown in figure 9, the cross-peaks in the two-dimensional NMR fingerprint regions are well dispersed and could be unambiguously identified for spin system assignments in the TOCSY spectrum and for sequential connectivity in the NOESY spectrum. The uninterrupted sequential walk unequivocally confirms the peptide head-to-tail backbone and the amino acid sequence derived from MS-MS fragmentation and amino acid analysis. The structure was calculated from a total of 232 interprotonic distances derived from the NOESY spectra, including 103 sequential constraints.

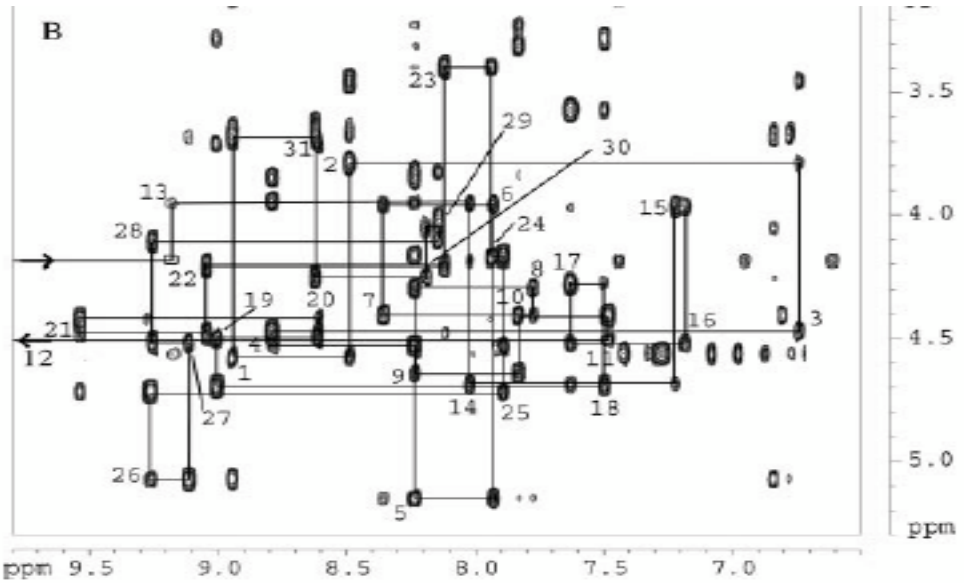

Figure 11: NOESY spectrum of Alba2

***Then, De novo* of Sequence Alba2 is VIGCSCKNKVCYLNSISCVSECAMISFCFTE**

3.3. Identification of Alba3

As for Alba1, Alba 2 structure was elucidated following the same procedure. The structure of this cyclotide was elucidated by de novo sequencing, comprising the analysis of a combination of single and multiple trypsin (blue arrows, dotted line), chymotrypsin (green arrows, dashed lines) and GluC endoproteinase (endothelialin) GluC, red lines, solid line) digests. The tandem mass spectra of (A) endo-GluC digestion and (B) digestion with trypsin are illustrated by way of example. The amino acid sequence was determined by manual assignment of the N- terminal b-ion and C-terminal ion series and the ion fragmentation calculation tool (Data Explorer ™, AB Sciex), (Figure 11) The complete sequence was determined by assembling the sequence fragments by interpretation of the digestion fragments using a combination of trypsin and chymotrypsin (left panel) and endo- GluC and chymotrypsin (right panel). The fragments of the different condensates are indicated by arrows. The masses labeled in the spectra relate to monoisotopic [M + H].

3.4. Identification of Alba3 and Alba4 by comparison

Amino acid sequences of purified cyclotides of Alba3 and Alba4 were obtained using an optimized MALDI- based peptidomics approach, termed 'sequence fragment assembly' [10]. The overall workflow is illustrated for Alba3 (Figure 11) and shown for other *De novo* sequenced cyclotides. The same method was used for elucidation of Alba4. First, the peptide was chemically modified to yield S-carbamidomethylation of cysteines, including the reduction of disulfide bonds with dithiothreitol, and the alkylation of reduced sulfhydryl groups with iodo-acetamide, which yielded a mass shift of 348.1 Da, indicative of the presence of six cysteine residues. Afterward, the fully reduced and alkylated peptide was digested with a single trypsin or endo-GluC to produce linear peptide chains amenable to fragmentation by MS/MS. The resulting spectra were analyzed manually by allocating N-terminal b- and C-terminal y-ions. Due to the presence of only one conserved glutamic acid residue in the cyclotide sequence, an endo-GluC digest will usually provide a complete C-N ion series of the linearized precursor ion. Single and double digests combining trypsin, endo-GluC and chymotrypsin were applied to generate smaller fragments with distinct molecular weight. By combining the annotated sequence information obtained from the molecular weight of fragments and alignment with the assigned endo-GluC ion series, it was possible to assemble the full cyclotide sequence of Alba3. The combination of trypsin/chymotrypsin (1338.5,
1450.6, and 1917.8 Da) and endo-GluC/chymotrypsin provided each three distinct fragments (1001.3, 2129.2, and 2622.5 Da). Each full length sequence was generated by alignment of the sequenced endo-GluC and tryptic ion series, with the annotated fragments of the trypsin/chymotrypsin and endo-GluC/chymotrypsin digest. Finally, sequences were confirmed by automated ion fragmentation analysis, chymotrypsin fragmentation pattern, sequence homology, and amino acid analysis. All these step uses for structure elucidation are summarized in figures 12, and figure 13 below. Then, De novo sequence ofAlba3: GIPCGESCVWIPCISSAIGCSCKGSKVCYRN and De novo sequence of Alba4 is GVIPCGESCVFIPCITAAI-GCSCKKKVCYRN , similar to Kalata B1 sequence in cyclotide from the root powder of the South American medicinal plant *Carapichea ipecacuanha* (Rubiaceae) screened by M. Fahradpour and his colleagues in 2017 [11].

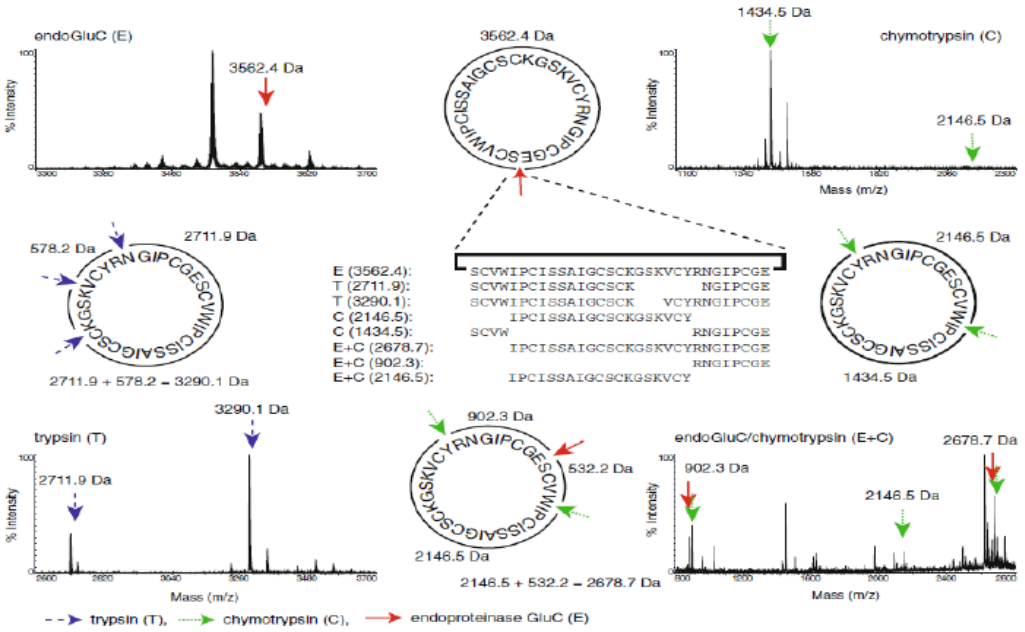

Figure 12: Sequence fragment assembly approach for Alba3

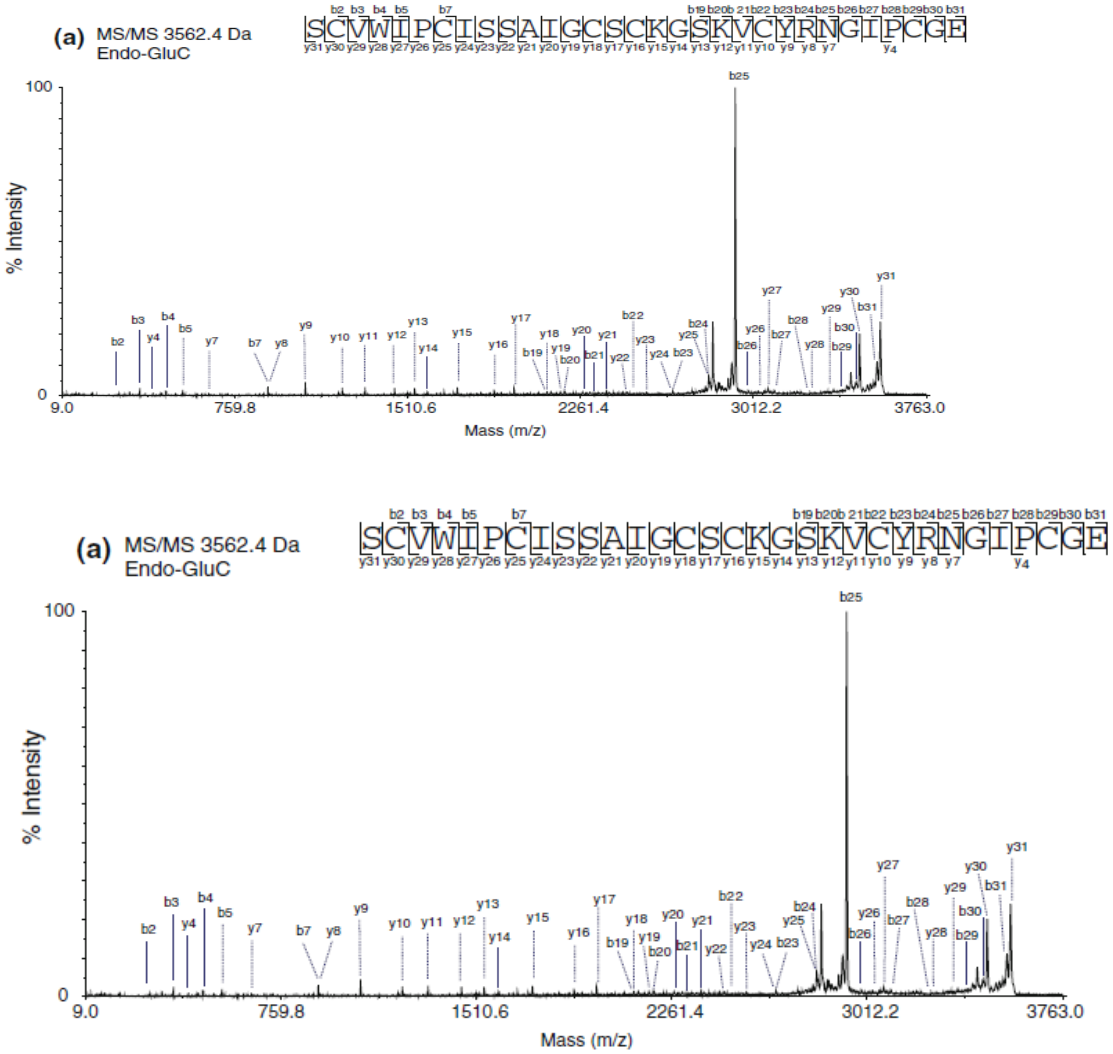

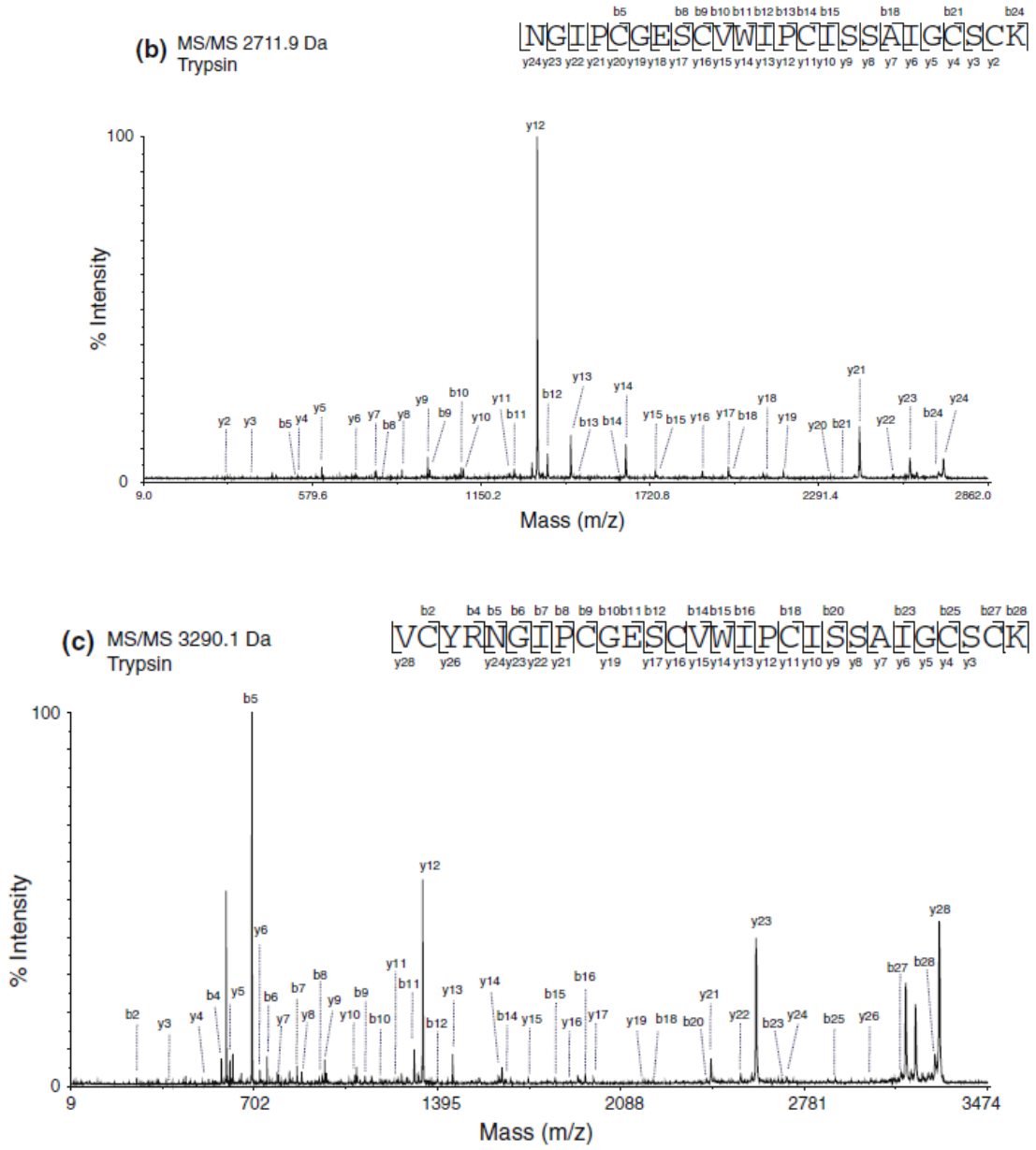

Figure 13: MS/MS sequence of Alba3

3.5. Supporting Information

The data of cyclotide Alba 4 are presented in supporting information; there are: MS / MS spectrum of the first fragmentation of Alba4 (Figure 14; MS / MS spectrum of second fragmentation of Alba4 (Figure 15); MS / MS spectrum of the third fragmentation of Alba4 (Figure 16); TOCSY spectrum of Alba4 (Figure 17), NOESY spectrum of Alba4 'Figure 18); Structure of Alba4 (Figure 19)

3.6. Membrane binding properties

3.6.1. Cyclotides permeabilization of lipid membranes

One of the objectives in this study was to understand membrane permeabilization properties of the two new cyclotides, Alba1 and Alba3 seen that samples of Alba3 and Alba4 were very few. The permeabilization ability of selected cyclotides was determined using a membrane leakage assay. In agreement with previous studies, there has been significant correlation observed between the ability of cyclotides to bind model membranes, as examined by SPR and ability to disrupt vesicles, as monitored by fluorescence measurements

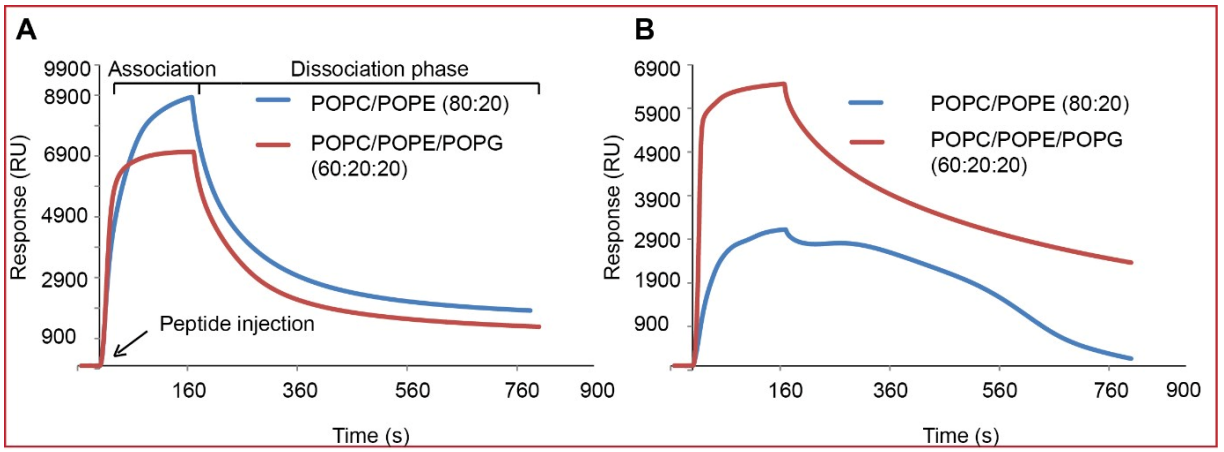

Figure 13: Comparison of binding ability of Alba1 Alba2 to PE-phospholipids.

Sensorgrams obtained with (A) Alba1 and (B) Alba2 injected over phospholipid bilayers composed of different lipid mixtures followed by SPR analysis are presented in figure 13. For a comparison, the amount of peptides bound to lipid bilayers was evaluated at 16 µM at the end of association phase (160 s of peptide injection). The dissociation phase for both the peptides was followed for 600 s. Results are mentioned in table 1 below.

Table 1: Membrane binding and vesicle permeabilization properties of cyclotides.

	POPC/POPE (80:20)			**POPC/POPE/POPG (80:20:20)**		
	P/L max[a] (mol/mol)	*Kd* (µM)[b]	LC50c (µM)	P/L max (mol/mol)	*Kd* (µM)[b]	LC50 (µM)
Alba3	0.15 ± 0.01	24.5 ± 1.44	4.87 ± 0.93	0.20 ± 0.01	22.55 ± 1.06	7.46 ± 0.59
Alba2	0.3 ± 0.01	6.82 ± 0.35	0.56 ± 0.05	0.31 ± 0.00	4.32 ± 0.09	1.02 ± 0.23
Alba1	0.13 ± 0.01	7.47 ± 0.86	0.30 ± 0.04	0.29 ± 0.00	4.99 ± 0.19	0.41 ± 0.12

It is interesting to note that all cyclotides showed no binding or very weak binding even in the presence of negatively-charged membranes. The binding potential of all cyclotides was quantified based on peptide-to-

lipid molar ratios (P/L) and *Kd* (dissociation constant, concentration required to achieve half-maximal binding at equilibrium)

3.6.2. Discussion

The mode of action of the three obtaining cyclotides was evaluated on a range of model membranes systems using a combination of SPR measurements, fluorescence studies and cryo-TEM imaging. The results from the SPR and fluorescence studies unequivocally support previous studies that cyclotides target and disrupt lipid membranes [10]. Phosphocholine (PC)-containing phospholipids are the most abundant phospholipids in eukaryotic cell membranes. Hence, in the current study, model membranes were prepared with POPC as a major component, due to the fact that it forms zwitterionic phospholipid bilayers in fluid phase at room temperature (25^{o}C) [12, 13]. All the selected cyclotides showed very weak or no binding to POPC lipid bilayers. To observe, the influence of negative charge on affinity of cyclotides, POPG, a phospholipid containing an anionic headgroup was added. It is interesting to note that all cyclotides showed no binding or very weak binding even in the presence of negatively-charged membranes. The binding potential of all cyclotides was quantified based on peptide-to-lipid molar ratios (P/L) and *Kd* (dissociation constant, concentration required to achieve half- maximal binding at equilibrium) resulted in an enhanced affinity for POPC/POPE/POPG with a *Kd* of 12.28
µM. This suggests the involvement of electrostatic attractions between negatively charged PG-head groups and the molecular surface of cyclotides with more positively charged residues. Regardless of sequence diversity, all cyclotides from both subfamilies exhibited identical specificity towards PE-containing phospholipids compared to other lipids. It should be noted that compared to bracelet members, Möbius members showed lower affinity for the tested model membranes.

4. Conclusion

In summary, this work reported the identification of cyclotides occurring in roots of *Allexis batangea* (Violaceae). Three new cyclotides, named Alba1, Alba2, Alba3, as well as one known Alba4 was purified and characterized by MALDI-MS/MS analysis, employing *de novo* sequencing and amino acid analysis. The other analysis data of cyclotide Alba 4 such as MS / MS spectrum of the first fragmentation, MS / MS spectrum of second fragmentation, MS / MS spectrum of the third fragmentation, TOCSY spectrum, NOESY spectrum and the structure of Alba4, are available as Supporting Information.

The present study also explored the mode of action of cyclotides through a combination of membrane binding, permeabilization studies and cryo-TEM imaging; regardless of sequence diversity, phospholipids containing PE- headgroups are essential for the ability of cyclotides to bind model membranes. Overall, the studies described in this publication have provided new insights into the molecular basis of cyclotide action. Although much remains to be done in this field to understand the full extent of cyclotide membrane interactions, the work described here provides a good resources.

Acknowledgement

All the Authors thank Mr Nana, Botanist at the National Herbarum Cameroon (NHC), for the collection & identification of plant material and the University of Kwazulu-Natal South Africa for his assistance in the method of extraction.

Conflict of Authors

Authors declare no conflict of interest

References

[1]. D.J. Craik, N.L. Daly, T. Bond, C. Waine. Plant cyclotides: a unique family of cyclic and knotted proteins that defines the cyclic cystine knot structural motif, J. Mol. Biol., 1999, Vol. 294, pp. 1327- 1336.

[2]. J. Weidmann and D.J. Craik. Discovery, structure, function, and applications of cyclotides: circular proteins from plants. Journal of Experimental Botany, 2016, Vol. 67(16), pp. 4801–4812. doi:10.1093/jxb/erw210.

[3].G. Poth, J.S. Mylne, J. Grassl, R.E. Lyons, A.H. Millar, M.L. Colgrave, D.J. Craik, .Cyclotides Associate with Leaf Vasculature and Are the Products of a Novel Precursor in Petunia (Solanaceae), J. Biol. Chem., 2012, Vol. 287, pp. 27033-27046.

[4a]. A A.G. Poth, M.L. Colgrave, R.E. Lyons, N.L. Daly, D.J. Craik. Discovery of an unusual biosynthetic origin for circular proteins in legumes, Proc. Natl. Acad. Sci., 2011, Vol. 108, pp. 10127-10132.

[4b]. A.G. Poth, M.L. Colgrave, R. Philip, B. Kerenga, N.L. Daly, M.A. Anderson, D.J. Craik. Discovery of cyclotides in the Fabaceae plant family provides new insights into the cyclization, evolution, and distribution of circular proteins, ACS Chem. Biol., 2011, Vol. 6, pp. 345-355.

[5] R. Hellinger; J. Koehbach; D. E. Soltis; E. J. Carpenter; G. K. Wong; and C. W. Gruber. Peptidomics of circular cysteine-rich plant peptides: analysis of the diversity of cyclotides from Viola tricolor by transcriptome and proteome mining. J. Proteome Res. 2015b, Vol. 14, pp. 4851–4862.

[6] G. Achoundong. The African genus Allexis (Violaceae). A synoptic revision, National Herbarium Cameroon, 2010, 9p.

[7] R. Burman, M.Y. Yeshak; S. Larsson; D.J. Craik; K.J. Rosengren and U. Göransson. Distribution of circular proteins in plants: large-scale mapping of cyclotides in the Violaceae. Front. Plant Sci. 2015, 6:855. doi: 10.3389/fpls.2015.00855.

[8] A. Dickey and R. Faller. Examining the Contributions of Lipid Shape and Headgroup Charge on Bilayer Behavior. Biophysical Journal, 2008, Vol. 95, 2636–2646.

[9] K. A. Babu and B. Jaykar. Development and Validation of Reverse phase high performance liquid chromatography method for simultaneous estimation of Paracetamol and Nabumetone in tablet dosage form Der Pharmacia Sinica, 2011, Vol. 2(5), pp. 192-197.

[9] C. K. Wang; H.P. Wacklin and D. J. Craik. Cyclotides insert into lipid bilayers to form membrane pores and destabilize the membrane through hydrophobic and phosphoethanolamine-specific interactions. Chem., 2012, Vol. 2012, pp. 1-28. DOI 10.1074/jbc.M112.372011.

[10] S. T. Henriques; Y.-H. Huang; M. A. R. B. Castanho; L. A. Bagatolli; S. Sonza; G. Tachedjian; N. L. Daly and D. J. Craik. Phosphatidylethanolamine Binding Is a Conserved Feature of Cyclotide-Membrane Interactions. The Journal of Biological Chemistry 2012, vol. 287(40), Pp. 33629-33643.

[11] M. Fahradpour; P. Keov; C. Tognola; E. Perez-Santamarina; P.J. McCormick; A. Ghassempour and C. W. Gruber. Cyclotides Isolated from an Ipecac Root Extract Antagonize the Corticotropin Releasing Factor Type 1 Receptor. Front. Pharmacology, 2017, vol. 8, pp. 1-14. doi: 10.3389/fphar.2017.00616.

[12] S. Zhu; M.-A. Sani; F. Separovic. Interaction of cationic antimicrobial peptides Australian de frogs with lipidic membranes. Peptide Science, 2018, vol. 110 (3), e24061.

[13] L. D. Daleke and W. H. Huestis. Erytrocyte Morphology Reflects the transbilayer distribution of incorporation phospholipids. jcb.nopress.org , 1989, 1375-1385 (16 March 2019)